Scientific Research Publishing

Journal of High Energy Physics, Gravitation and Cosmology, 2024, 10, 106-125
https://www.scirp.org/journal/jhepgc
ISSN Online: 2380-4335
ISSN Print: 2380-4327

Hubble Tension Explanation from This Cosmological Model ΑΛΩ (Slow Bang Model, SB)

Jean Perron

Department of Applied Sciences, Université du Québec à Chicoutimi, Saguenay, Canada
Email: jean_perron@uqac.ca

How to cite this paper: Perron, J. (2024) Hubble Tension Explanation from This Cosmological Model ΑΛΩ (Slow Bang Model, SB). *Journal of High Energy Physics, Gravitation and Cosmology*, **10**, 106-125.
https://doi.org/10.4236/jhepgc.2024.101010

Received: September 5, 2023
Accepted: January 12, 2024
Published: January 15, 2024

Abstract

In this article we present a model of Hubble-Lemaître law using the notions of a transmitter (galaxy) and a receiver (MW) coupled to a model of the universe (Slow Bang Model, SB), based on a quantum approach of the evolution of space-time as well as an equation of state that retains all the infinitesimal terms. We find an explanation of the Hubble tension H_0. Indeed, we have seen that this constant depends on the transceiver pair which can vary from the lowest observable value, from photons of the CMB (theoretical $\sim 68.32^{+0.49}_{-0.47}$ [km/s/Mpc]) to increasingly higher values depending on the earlier origin of the formation of the observed galaxy or cluster (ETG ~0.3 [Gy], ~74 [km/s/Mpc]). We have produced a theoretical table of the values of the constant according to the possible pairs of transmitter/receiver in the case where these galaxies follow the Hubble flow without large disturbance. The calculated theoretical values of the constant are in the order of magnitude of all values mentioned in past studies. Subsequently, we applied the models to 9 galaxies and COMA cluster and found that the models predict acceptable values of their distances and Hubble constant since these galaxies mainly follow the Hubble flow rather than the effects of a galaxy cluster or a group of clusters. In conclusion, we affirm that this Hubble tension does not really exist and it is rather the understanding of the meaning of this constant that is questioned.

Keywords

Model of the Universe, Cosmological Constant, Hubble Constant, Hubble's Tension, Hubble-Lemaître Law, Hubble's Flow

1. Introduction: The Hubble Tension?

For some time, in fact, since we have been measuring the Hubble constant more

accurately, we have observed significant variations in the measurement of it. A large number of articles present these measurements of this constant and the methods used are as varied as they are original (Cepheids-SN1a, CMB, BBN, TRGB, BAO, etc.) This article is not a review of the measurements made in recent years, let alone a criticism of the methods used. We refer to [1] [2] which present a comprehensive review of the different measures and methods in recent years as well as several explanations as different from each other on the origin of the Hubble tension (more than 120 different explanations!). In fact, we will see in this article that all these measures are actually good proportionally to the precision of the method used and for a specific source of photons (galaxy or body). We will see that the constant H_0 depends and varies mainly with the source from which the photons come and the origin of this source from the beginning (time of formation or beginning of photon emission). Thus, we will find that this so-called Hubble tension does not really exist and that the most universal Hubble constant H_0 which is the one measured at our space-time MW can be derived from the earlier transmitted signal as the CMB photons with a model of galaxies or bodies origin time (as for the MW) since the expansion of the universe.

2. Fundamental Model of the Expansion of the Universe Based on Hubble Constant Definition and Notion of Signal Issuer Receiver (Photons Propagation)

In this section, we develop a model for predicting the Hubble constant with the concept of a source (the transmitter) and a receiver which is for us the MW. The model is based on the following assumptions:

1) The notion of the expansion of the universe, grouped around the Hubble-Lemaître law with H_0 and FLRW metric is based on the measurement of a signal emitted (the transmitter) to a signal received (the receiver). The current signal is the propagation of photons at velocity c.

2) At our space-time of the MW, (the receiver), we have the possibility to measure several signals (several values of H_0) according to the origin of the various galaxies observed (various transmitters). All these values are relative to the transceiver pair (MW and galaxy pair).

3) The different H_0 values measured are all good and valid for each of the pairs in question with the exception of galaxies which are subject to significant additional effects of gravity of surrounding bodies which modifies accordingly the measured value (acceleration or deceleration or peculiar velocity).

4) The intrinsic or unique theoretical H_0 value that does not depend on the transceiver pair cannot be measured in absolute from the MW (universal cosmic observer) but derived from that measured from MW (MW observer).

5) The best theoretical value from the MW is the one measured from the first photons emitted from the CMB (MW-CMB pair).

6) In summary, when we estimate H_0 values from different surrounding galaxies, we produce a table of H_0 (along a space-time line) relating to the origin time and evolution of the observed galaxies.

We could produce a theoretical XY table of H_0 with the origin time of formation of the transmitter and origin time of formation of the receiver. The origin time of formation will be determined with a model already developed few years ago and already published in this journal (see next section).

The Hubble-Lemaître law between a transmitter (2) and a receiver (1) isolated in a universe in constant expansion (uniformly accelerated motion) and not relativistic with the recession velocities between the transmitter (2) and the receiver (1) (max~30,000 km/s or <0.1*c*) is expressed as:

$$v(t)=v_2(t)-v_1(t)=H(t)d(t)=H(t)\left(r_2(t)-r_1(t)\right)$$

or:

$$H(t)=\frac{v_2(t)-v_1(t)}{r_2(t)-r_1(t)}=\frac{\Delta v_{helio}}{\Delta r_{helio}}$$

With the well-known expressions of uniformly accelerated motion, we find

$$H(t)=\frac{v_{02}-v_{10}+\overline{a}\left(t_1'-t_2'\right)}{d_{20}-d_{10}+v_{02}\left(t-t_2'\right)-v_{01}\left(t-t_1'\right)+\frac{\overline{a}}{2}\left(t_1'^2-t_2'^2\right)}$$

With

$$\overline{a}=\frac{v_1(t)-v_{01}}{t-t_1'}=\frac{v_2(t)-v_{02}}{t-t_2'}$$

$$v_{02}=\left(v_2-v_1\right)-\overline{a}\left(t_1'-t_2'\right)+v_{01}$$

$$d_{20}-d_{10}\sim\left(v_{02}-v_{10}\right)\left|\left(t_1'-t_2'\right)\right|$$

t: age of universe (13.8 [Gy]) [s].

d_{01} : distance to origin of the receiver (1) [km].

v_{01} : velocity at the origin of the receiver (1) [km/s].

t_1' : time at the end of main formation of the receiver (1) [s].

d_{02} : distance to origin of the transmitter (2) [km].

v_{02} : velocity at the origin of the transmitter (2) [km/s].

t_2' : time at the end of main formation of the transmitter (2) [s].

$\overline{a}$: mean constant acceleration of bodies [km/s^2].

H: Hubble constant perceived by receiver (1) [s^{-1} or 3.08569 × 10^{19} km/s/Mpc].

In the equations above, we see that if we estimate the times, distances, starting velocities of bodies (1) and (2), the mean acceleration as well as the total acceleration time, we can estimate the Hubble constant perceived by the body (1) vis-à-vis the body (2). The body (1) will be the MW and the body (2), the observed galaxy. We must know at least the approximate time of the main formation of the galaxy (2) (t_2'). The model described in the following section makes it possible to estimate these parameters for a particular galaxy by knowing the baryonic mass of that galaxy and its measured rotational velocity profile as well as by adjusting the theoretical rotational velocity profile using the knowledge of the cosmological constant $\Lambda\left(t_2'\right)$ that which represents the surrounding energy at the formation

time t_2' of this galaxy (2). Surrounding energy that participates in the curvature of space-time around this galaxy (see next section). By estimating all the parameters of the Hubble-Lemaître equation, it will be possible to estimate the evolution of the constant H_0 along the space-time line of this galaxy (2) vis-à-vis MW (1).

We can use the above equations and evaluate the theoretical Hubble constant for the CMB (located at about $t_2' = 0.0004$ Gy and $v_{02} = c$) as well as for observed galaxies ETG and other less old LTG up to much higher values of their formation time around $t_2' = 5$ Gy VLTG. We obtain Table 1. Note that the values of the constant H_0 are theoretical, that is, the transceiver pair is not influenced by the gravity of other surrounding bodies and the bodies (1) (the MW) and (2, galaxy) move according to the pure Hubble flow. Also, for comparison purposes, the relative velocities $v_2 - v_1$ are constant at 1000 [km/s].

The results obtained are remarkable and several conclusions can be drawn from the values obtained. Key observations and conclusions include:

1) The developed model of the prediction of the Hubble constant indicates that the values of H_0 from a cosmic observer depend on the space-time of this observer as well as the observed galaxy is the transceiver pair.

Table 1. Theoretical Hubble constant H_0 from above eq. of a transceiver pair following the Hubble flow in an isotropic FRLW universe with formation of structure. The first horizontal line (gray) corresponds to the theoretical value H_0 (galaxy, CMB) for different galaxies according to their formation time t_1'. The second vertical line (gray) corresponds to the H_0 (galaxy, CMB) for an observed galaxy from the MW moving at a constant velocity 1000 [km/s].

		Receiver (1) of photons (main time of formation, t_1' [Gy])												
							MW (0.52)	Xiang [4] Planck 2018						
		0	0.1	0.2	0.3	0.4	0.52	0.6	0.7	0.8	0.9	1	2	5
CMB	0.0004	70.9	70.39	69.89	69.39	68.9	**68.32**	67.94	67.48	67.01	66.56	66.11	61.92	52.04
	0.1	70.6	71.4	72.2	73.0	73.9	**74.8**	75.6	76.5	77.3	78.3	79.2	89.7	138.6
	0.2	68.9	72.47	71.94	71.42	70.90	**74.6**							137.6
	0.3	70.1	73.56	73.01	72.47	71.94	**74.3**							136.6
	0.4	69.9	74.69	74.12	73.56	73.01	**74.0**							135.6
	0.5	69.6	70.4	71.1	71.9	72.7	**73.7**	74.4	75.2	76.1	77.0	77.9	88.9	134.7
	0.6	69.4	77.04	76.44	75.84	75.26	**73.4**	74.13						133.9
	0.7	69.1	78.27	77.65	77.04	76.44	**73.7**		74.69					133.0
	0.8	68.9	79.54	78.9	78.27	77.65	**72.9**			75.26				132.1
	0.9	68.7	80.86	80.2	79.54	78.9	**72.7**				75.84			131.3
	1	68.4	82.22	81.53	80.86	80.2	**72.4**					76.44		130.5
	2	66.3	98.83	97.84	96.87	95.92	**70.0**						82.92	123.5
	5	61.6	62.2	62.8	63.5	64.1	**64.9**	65.4	66.1	66.8	67.5	68.2	76.1	111.1

Transmitter (2) of photons (main time of formation, t_2' [Gy])

ETG ← zone of observed galaxies → LTG

2) The observable values of H_0 from our point of view (MW observer) start with that of CMB photons (smallest observable value of photon at $v_{02} = v_2 = c$). Subsequently, as the relative velocity of galaxies decrease sharply, the range of observable values gradually decreases from 74.8 for ETG's to 64.9 LTG's, *i.e.* a variation of nearly 10 [km/s/Mpc].

3) With an accurate measurement of the Hubble constant made from CMB photons, it is possible to determine an approximate time of the main formation of MW. If we accept a value of 67.36 ± 0.54 [km/s/Mpc] (Planck alone) (Planck 2018, [3]), we find an approximate formation time of the MW from 610 to 840 [My] after the beginning, this range of values corresponds to that proposed ~800 [My] by Xiang [4]. This question of the formation time of a galaxy t_i' remains partly imprecise, if we consider a more or less long formation time and the moment when a cluster of matter becomes an organized galaxy or structure with its own mean motion v_i (Hubble flow).

4) The model largely explains the confusion surrounding the measured values of H_0. Indeed, the model shows that the observed values of ETG galaxies (younger than 0.2 [Gy]) can reach values as high as ~75 [km/s/Mpc].

5) The average value observed from the MW for all galaxies is around 72.6 +/-2.7 [km/s/Mpc]. This value is well in the middle of all the values mentioned in the various studies since 2013, excluding indirect measurements from CMB photons.

6) Based on the model as well as for an observer from the MW ($t_1' = 0.52$ [Gy]), the theoretical value of $H_0(\mathrm{MW},\mathrm{CMB})$ is ~68.32 [km/s/Mpc]. With a variation of ±100 [My] of $t_1'(\mathrm{MW})$ we find:

$$H_0(\mathrm{MW},\mathrm{CMB}) = 68.32^{+0.49}_{-0.47} \quad [\mathrm{km/s/Mpc}]$$

This value compares with this recent value:

$$H_0(\mathrm{SPT}-\mathrm{TT}/\mathrm{TE}/\mathrm{EE}) = 68.3^{+1.5}_{-1.5} \quad [\mathrm{km/s/Mpc}] \text{ [5]}$$

3. Model of Universe with a Specific Time of Formation t_i, t_b, t_t of Structures Like Galaxies and Clusters

It was in 2018 that the development of the model began and the first preprint publication appeared in [6]. Subsequently, in 2021 and 2023, 4 publications appeared in this journal [7] [8] [9] [10]. We refer the reader to these articles which contain all details. Here are some key elements of this model. At the beginning, at time 0, a first Planck volume and first photon $\hat{\gamma}$ s present and this is predicted by an equation (a photon in a quantum box). According to the model and the quantization of energy and space, photons are generated, at each Planck time, during ~10^{-9} [s] according to a progression close to $(n + 1)^3$, n being the Planck time number. Time and space evolve quantically in this model. The energy source causing photons generation is contained at the outer edge of the universe or from an unidentified internal source often referred to as vacuum energy. The number reached is about $6.4\times10^{89}\hat{\gamma}$. Thus, we see that the model considers an origin of

the "Bang" type but the "Big" is rather a relatively slow quantum evolution of energy creation is the expression Slow Bang, SB. The model evolves according to cosmic time and all the variables of the universe (more than 25) are dynamic and evolve according to cosmic time. This model does not need the inflation phenomena since energy generation is slow and in phases (causal) with the space generation (see [6]).

Here is a summary of the main elements of this model:

- Time and space evolve quantically (Planck step t_p, l_p).
- During the energy creation (~10^{-9} [s]), the quantum nature of photon creation is applied.
- The macroscopic laws of physics applied after this energy creation period.
- The law of conservation of energy applies to universe-size scales.
- The cosmological principle is not necessarily adhered to.
- The Hubble constant of the Hubble-Lemaître law is used to solve the Friedmann equations and find specific expression for $\Lambda(H)$ and $k(H)$. After some development, we find these expressions (see [6]):

$$k(H) \sim a^2 \left[9.61 \times 10^{16} H^4 + 3.04 \times 10^{-3} H^3 - 1.11 \times 10^{-17} H^2 \right] \left[\mathrm{m}^{-2} \right]$$

$$\Lambda(H) \sim 2.88 \times 10^{17} H^4 - 1.08 \times 10^{-1} H^3 \left[\mathrm{m}^{-2} \right]$$

4. Cosmological Gravity Force, F_Λ from Mass-Energy Equivalence and GR

For the time period when radiation was dominant, a central force associated with $\Lambda(t)$ can be determined using mass-energy equivalence. Indeed, we know the value of Λ via the evolution of energy in the universe. Let us assume an element with mass m in rotation according to a Kepler model in a central gravity field of mass M. Another attractive force is a work around mass m, this time associated with the non-baryonic energy density, which acts through mass-energy equivalence of the interior sphere whose boundary is determined by the rotation radius, r, of mass m.

In this model, we consider that the force is attractive simply through mass-energy equivalence, which can also be achieved with the GR (see below), meaning that a positive energy mass is associated with a positive energy, such as the energy of photons associated with constant Λ, and that energy exerts a space-time deformation on surrounding masses the same way the inertial mass (baryonic) does.

We can see that the mass-energy associated with the cosmological constant depends on a zone demarcated by the assumed radius, r. This can partially explain the issues with the cosmological constant, Λ. In fact, that gravity force can be put into action in the GR equation through the existence of the cosmological constant, as put forth by Einstein but for a different reason than the static universe he proposed. Indeed, the cosmological constant was later added by Einstein as an opposing force to gravity. Therefore, when the term $\Lambda g_{\mu\nu}$ is moved to the right-hand side, the side of the energy-momentum tensor, we get a repulsive effect associated with Λ:

$$R_{\mu\nu} - \frac{1}{2} R g_{\mu\nu} + \Lambda g_{\mu\nu} = \frac{8\pi G}{c^4} T_{\mu\nu}$$

with the signature of the metric tensor (+, −, −, −), the energy-momentum tensor can be expressed as:

$$T_{\mu\nu}^{total} = T_{\mu\nu}^{baryonic} - \rho_{\Lambda e} g_{\mu\nu}$$

In this case, the resulting force is repulsive, as Einstein wanted. However, it is also possible to make the effects of that energy appear directly in the energy-momentum tensor as a source of additional mass-energy through the mass-energy principle, as:

$$T_{\mu\nu}^{total} = T_{\mu\nu}^{baryonic} + T_{\mu\nu}^{mass\text{-}energy}$$

$$T_{\mu\nu}^{total} = T_{\mu\nu}^{baryonic} + \frac{E_\Lambda}{V} g_{\mu\nu}$$

$$T_{\mu\nu}^{total} = T_{\mu\nu}^{baryonic} + \rho_{\Lambda e} g_{\mu\nu} = \rho_m c^2 + \frac{c^4 \Lambda}{8\pi G} g_{\mu\nu}$$

Hence, the energy density component of the tensor, T^{00}, is entirely positive:

$$T^{00} = \rho_m c^2 + \frac{c^4 \Lambda}{8\pi G} = \rho_{m+\Lambda} c^2$$

The solution for the spherical geometry is found in the Newton equation for low velocities:

$$\nabla^2 \Phi = 4\pi G \rho_{m+\Lambda} = 4\pi G \left(\rho_m + \frac{c^2 \Lambda}{8\pi G} \right) = 4\pi G \rho_m + \frac{c^2 \Lambda}{2}$$

The potential being:

$$\Phi = -\frac{Gm}{r} + \frac{c^2 \Lambda r^2}{12}$$

$$\boldsymbol{a} = -\frac{Gm}{r^2} \boldsymbol{e}_r - \frac{\Lambda}{6} c^2 r \boldsymbol{e}_r$$

We can see that, at this time, solving the equation predicts an attractive force associated with constant Λ and of the same type as the baryonic mass. The r term can be related to the Hooke ellipse.

$$\Phi(m, r, H) = -\frac{Gm}{r} + \frac{c^2 k_\Lambda}{12} H^4 r^2$$

Then, solving the equation for low velocities (Newton) includes one mass contributors (baryonic) and one energy (k_Λ, cosmological). The geometric variable r of the structure and the time factor of formation of the structure H (*or 1/t*).

Therefore, assuming this notion of mass-energy, and according to Newton's law of attraction for that mass, m_Λ, the central attractive force associated with the mass-energy equivalence can be written as:

$$|F_\Lambda| = \frac{G m_\Lambda m}{r^2} = \frac{G(\rho_\Lambda V) m}{r^2} = \frac{G(\rho_\Lambda 4\pi r^3) m}{3r^2}$$

$$= \frac{4\pi G(\rho_\Lambda) r m}{3} = \frac{4\pi G}{3} \left(\frac{c^2 \Lambda}{8\pi G} \right) r m = \frac{\Lambda}{6} c^2 m r$$

5. Some Galaxies Rotation with Baryons and Λ(*t*)

In this section, we present only the equations used. For a given circular rotation orbit, the tangential rotation velocity of a mass is expressed through the balance of the main forces considered in the model: Newtonian gravity and cosmological gravity via mass-energy equivalence:

$$F_c = F_G + F_\Lambda$$

$$m\omega^2 r = Gm\left(\frac{M}{r^2} + \frac{\Lambda c^2 r}{6G}\right)$$

$$v_t^2 = G\frac{M}{r} + \frac{\Lambda c^2 r^2}{6}$$

For a galaxy, the masses of the bulb and disc, we get a simplified expression:

$$M_T(r,t) = M_b(r,t) + M_d(r,t)$$

$$M_T(r,t) = \frac{V_b(r,t)}{V_{b_T}}M_b + \frac{V_d(r,t)}{V_{d_T}}M_d = \frac{r(t)^3}{r_b^3}M_b + \frac{r(t)^2 - r_b^2}{r_T^2 - r_b^2}M_d$$

where:

$0 \le r(t) \le r_b$, for the bulb;

$r_b \le r(t) \le r_T$, for the disc;

r_b: bulb radius determined at the end of galaxy formation;

r_T: disc and bulb radii determined at the end of galaxy formation;

M_b: bulb mass determined at the end of galaxy formation;

M_d: disc mass determined at the end of galaxy formation.

A simple law can be used to calculate mass accumulation at a constant rate:

$$r(t) = \alpha t = \frac{t}{t_T - t_i}r_T$$

where

$t_i \le t \le t_t$, formation time of the galaxy;

α: galaxy radius growth rate (accumulation).

For the mass, we get:

$$M_T(r,t) = \frac{\alpha^3 t^3}{r_b^3}M_b + \frac{\alpha^2 t^2 - r_b^2}{r_T^2 - r_b^2}M_d$$

Finally, for rotation velocity, we get:

$$v_t^2 = G\left[\frac{\alpha^2 t^2}{r_b^3}M_b + \frac{\alpha^2 t^2 - r_b^2}{\alpha t\left(r_T^2 - r_b^2\right)}M_d\right] + \frac{k_\Lambda c^2 \alpha^2 t^2}{6(t + t_i)^4}$$

where

$t_i \le t \le t_t$, formation time of the galaxy;

$t_i \le t_b \le t_B$: formation time of the galaxy bulb;

$t_B \le t_d \le t_t$: formation time of the galaxy disc;

t_i: age of the universe at the time of galaxy formation to calculate.

$$\Lambda(t)=\frac{k_\Lambda}{(t_i+t)^4}=k_\Lambda H^4,$$

with

$$k_\Lambda=\left[\frac{32\pi G\sigma C_1^4}{c^5}\right]=\left[\frac{32\pi G\sigma T_\Omega^4 t_\Omega^4}{c^5}\right]=2.88\times10^{17}\left[\mathrm{s}^4\cdot\mathrm{m}^{-2}\right]$$

This equation contains the essential elements for predicting the rotation curve of the luminous mass of galaxies. In [6] [7] [8] [9] [10] we have already used this rotation equation for some galaxies. Here are the curves obtained for more galaxies. The choice of these galaxies is arbitrary but some of them have special characteristics (size, with or without DM, UDG, SMBH). They are located close to us (NGC253 3 Mpc) or much further (UGC12591, 75 to 144 Mpc). The data come mainly from the NED, SIMBAD databases but also from various articles.

What we find in [10] is special. Indeed, according to the model, most galaxies are formed much earlier than the predictions of conventional models for predicting galaxy formation as seen for some galaxies with JWST. As an example, the MW to start the formation of the bulbs 180 to 200 [My] after the beginning. In addition, the evolution time is much faster than is normally envisaged. Here are the times since the beginning of the formation and the evolution time of the main formation of galaxies studied. Of course, nothing prevents the internal reorganization of galaxies by collisions and other phenomena throughout the history of galaxies. For the MW we find:

MW, begin 180 - 200 [My],

Formation time ~320 [My],

Main structure t_1' ~520 [My],

Intrinsic velocity relative to CMB v_{01} ~50 [km/s] ([6]],

Intrinsic velocity relative to CMB $v_1 = v_{LG}$ ~620 [km/s] [11],

Intrinsic acceleration relative to CMB $\bar{a}$ ~42.92 [km/s/Gy].

Mean rotational tangential velocities (**Figure 1**, measured values, Blitz *et al.*, 1980 [12]).

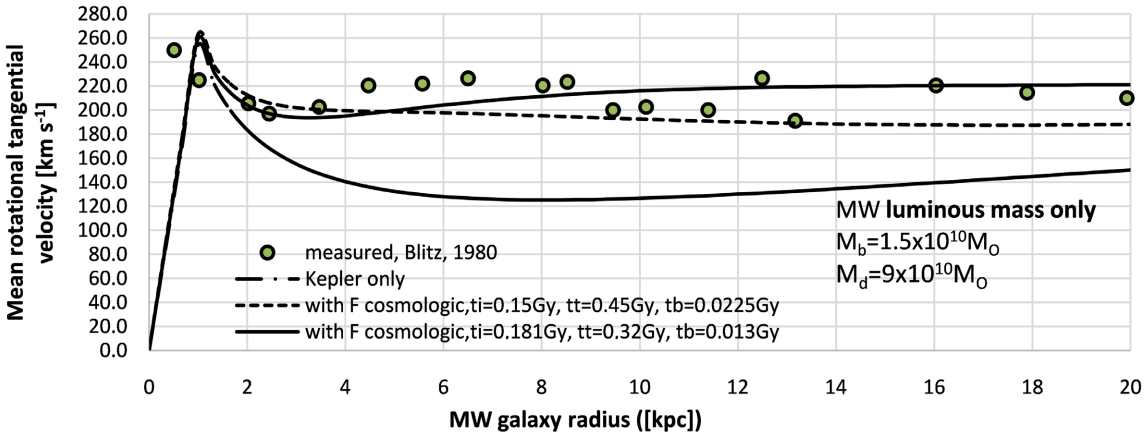

Figure 1. MW rotational velocities.

The following figures show the results obtained for the rotational velocity measured and predicted with the model using baryonic mass only for galaxies. Following this, the specific formation times of galaxies to be used in the H_0 model ($t' \sim t_i + t_t$) are shown from the rotation curves. We see that it is possible to estimate an approximate time of the beginning of the formation of a galaxy as well as the total time of the primary formation with the addition of this cosmological force (mass-energy equivalence) to gravity. However, it is difficult to determine when precisely a galaxy in the process of formation can be identified as possessing its proper motion or its motion according to the Hubble flow. In this model, we arbitrarily choose this period as the end of the main formation of the galaxy but when the formation is very long (~1 [Gy]) this value of t' may be less than the total formation time (~50%).

From these figures the following observations could be drawn which will be used for the prediction of the Hubble constant:

UGC12591, begin 170 - 180 [My], formation time 280 [My], main structure ~460 [My] (**Figure 2**, measured values, Giovanelli *et coll.*, 1985 [13]).

COMA cluster, begin 500 - 720 [My], formation time 1.5 [Gy], main structure ~2 [Gy] (**Figure 3**, measured values, Kent *et coll.*, 1982 [14], Rood *et al.*, 1985 [15], Chincarini *et al.*, 1976 [16]).

UDG 44 (Dragonfly), begin 180 [My], formation time 390 [My], main structure ~570 [My] (**Figure 4**, measured values, Van Dokkum *et coll.*, 2019 [17]).

UGC2885, begin 175 - 180 [My], formation time 1.2 [Gy], main structure done ~1.4 [Gy] (**Figure 5**, measured values, Gentille *et coll.*, 2013 [18]).

AGC114905, begin 500 [My], formation time 650 [My], main structure done ~1.15 [Gy] (**Figure 6**, measured values, Mancera Pina, 2022 [19]).

NGC4183, begin 220 [My], formation time 450 [My], main structure done ~670 [My] (**Figure 7**, measured values, Martins *et coll.*, 2007 [20], Stark *et al.* 2009 [21]).

DDO161, begin 220 [My], formation time 260 [My], main structure done ~460 [My] (**Figure 8**, measured values, Coté *et coll.*, 2000 [22]).

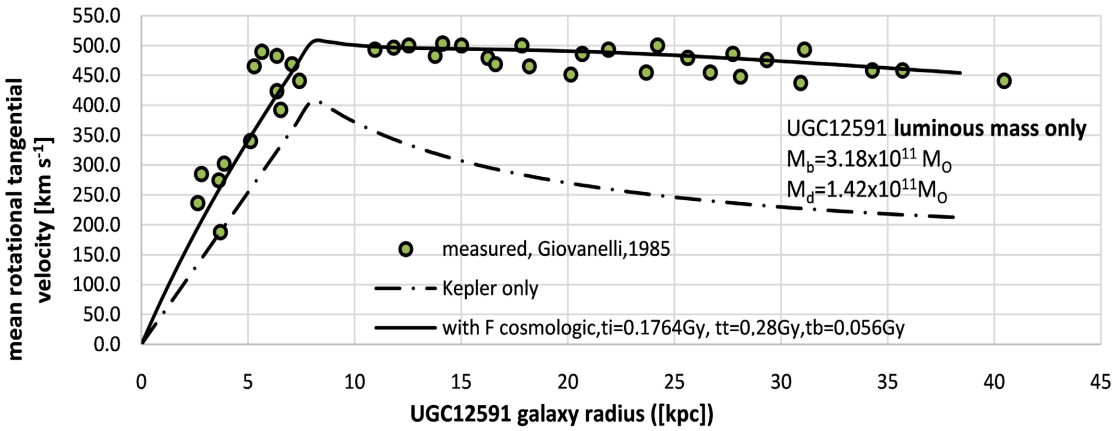

Figure 2. UGC12591 rotational velocities.

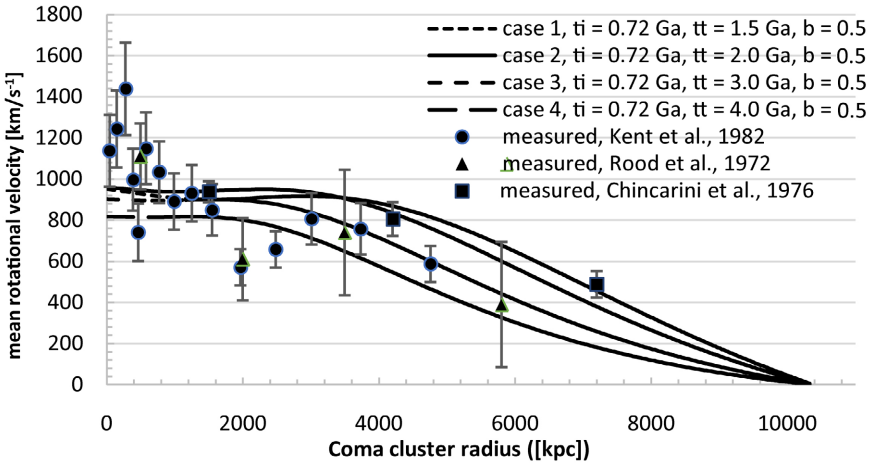

Figure 3. Coma cluster rotational velocities.

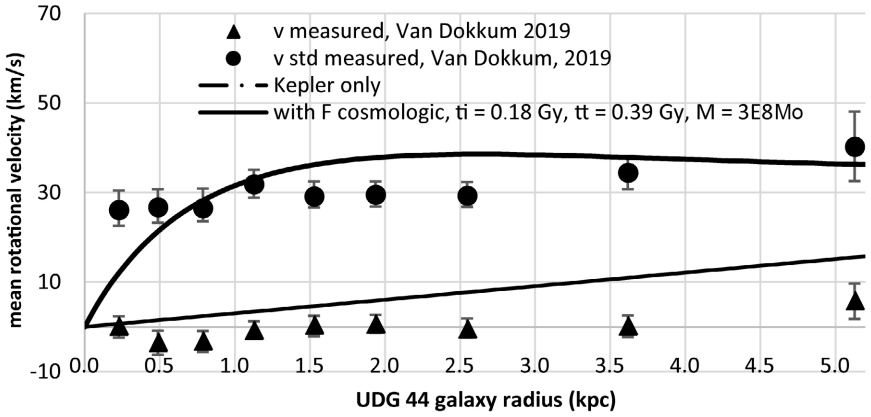

Figure 4. UDG 44 (Dragonfly) rotational velocities.

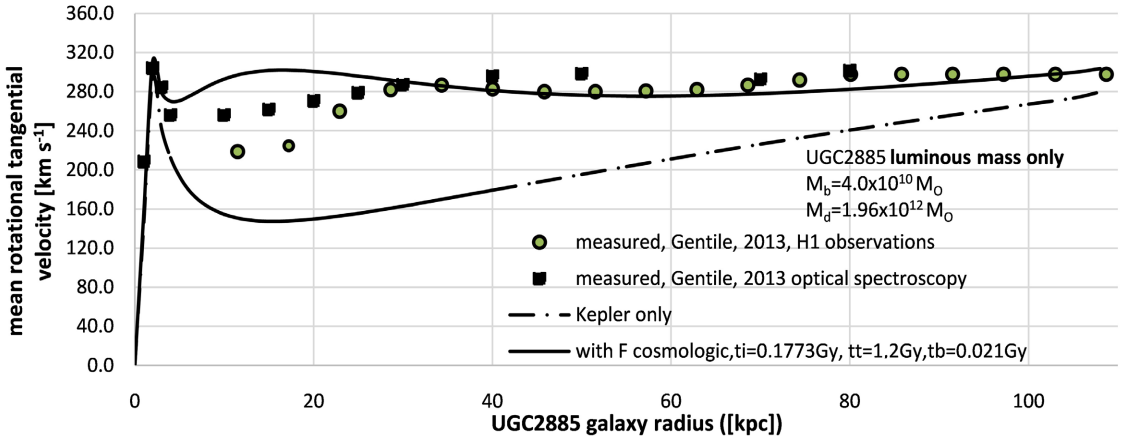

Figure 5. UGC2885 rotational velocities.

NGC3198, begin 180 - 185 [My], formation time 880 [My], main structure done ~1.1 [Gy] (Figure 9, measured values, Gentille *et coll.*, 2013 [18]).

NGC253, begin 175 - 180 [My], formation time 320 [My], main structure done ~500 [My] (Figure 10, measured values, Pence *et coll.*., 1981 [23]).

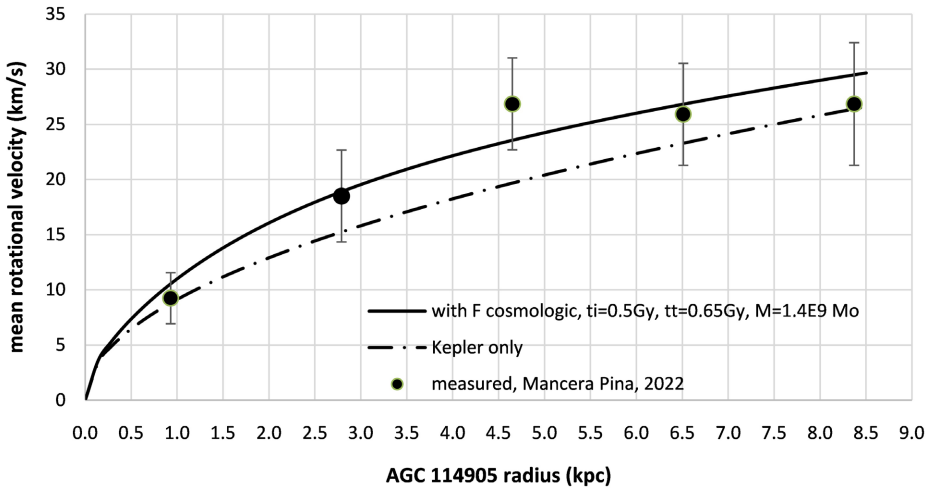

Figure 6. AGC 114905 rotational velocities.

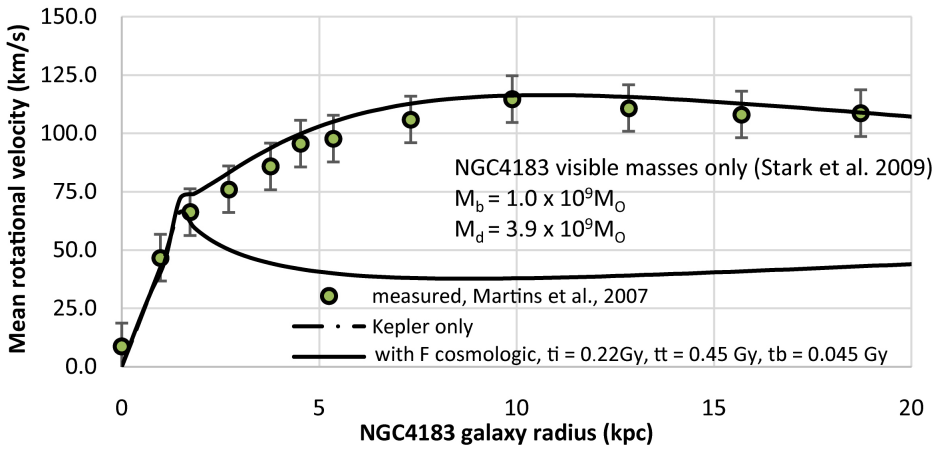

Figure 7. NGC4183 rotational velocities.

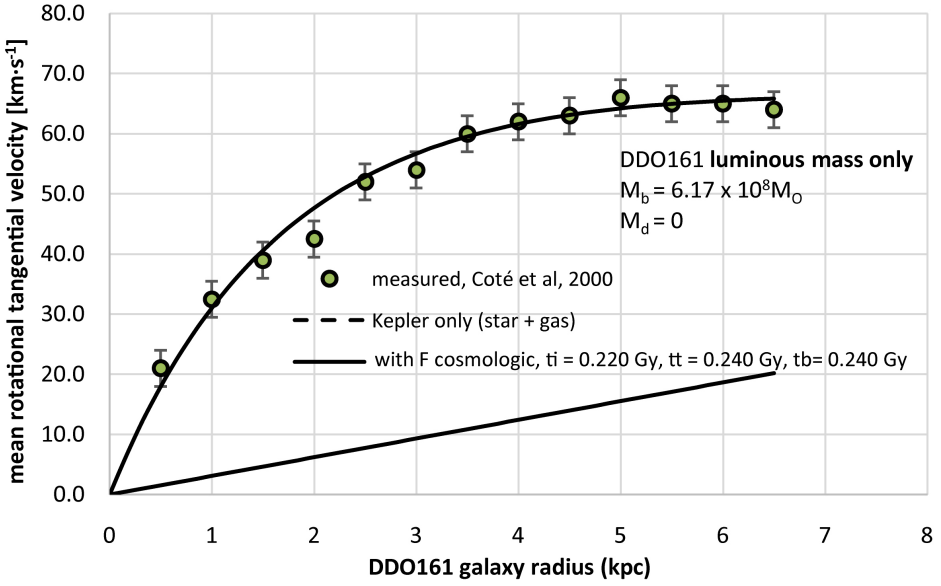

Figure 8. DDO161 rotational velocities.

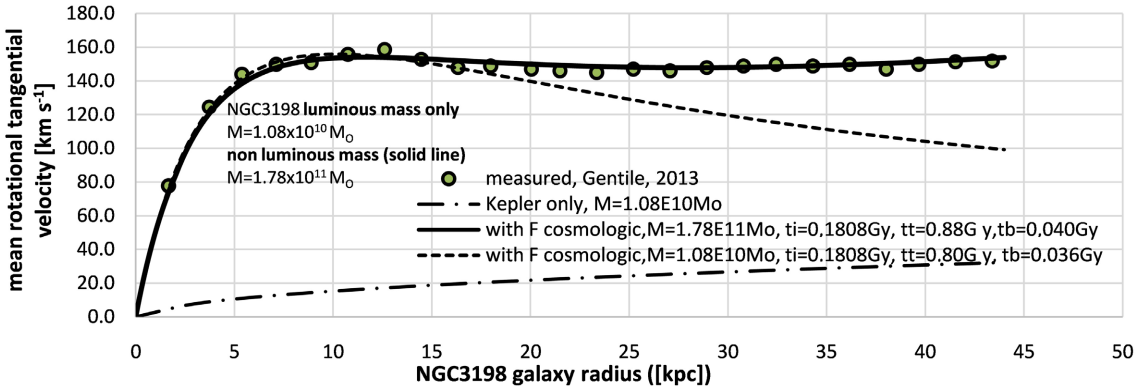

Figure 9. NGC3198 rotational velocities.

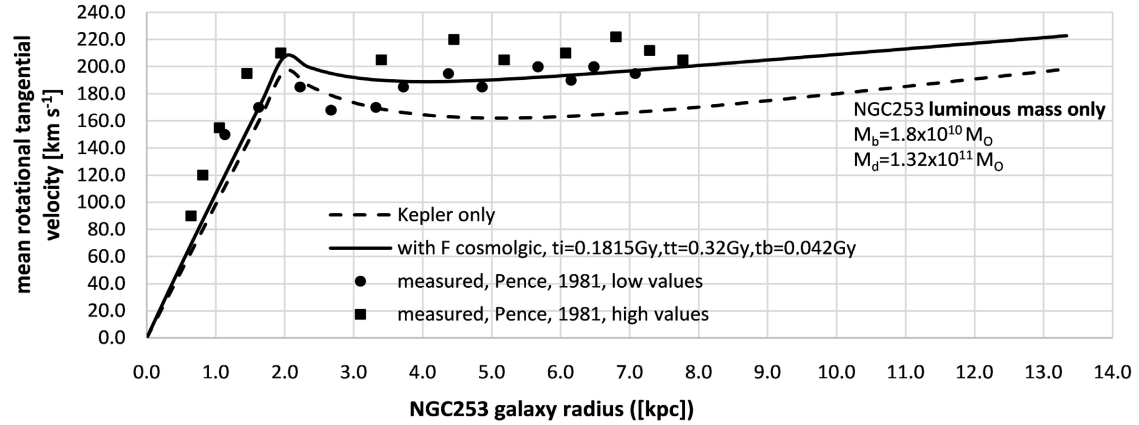

Figure 10. NGC253 rotational velocities.

M87, begin 120 [My], formation time 320 [My], main structure done ~440 [My] (Figure 11, measured values, Macchetto *et coll.*, 1997 [24]).

We see that an intense period of galaxy formation around 120 - 220 [My] after the beginning seems to exist, at least for galaxies near MW.

The following Table 2 presents the data for the 9 galaxies and COMA cluster studied as well as the predictions of the cosmological model and the value of the Hubble constant estimated with the measurements and that predicted by the transceiver model (receiver (1) MW).

Some observations emerge from Table 2.

1) The predicted theoretical value of $H_0(\mathrm{MW},\mathrm{CMB}) = 68.32$ [km/s/Mpc] (MW-CMB) pair is similar to those determined by the various studies using the CMB or the oscillation of baryons of a transmitting source less than 500 [ky] from the origin (Planck 2018, SDSS-III BAO 2016, SPT 3G 2023) (~67.3 to 68.3 [km/s/Mpc]).

2) Estimates of the Hubble constant for the galaxies studied vary depending on the source. Indeed, significant variations in the estimation of the distances of galaxies are mentioned (variation from singles to triple). However, the predicted values of the Hubble constant are for the majority of galaxies within or near the estimated limits.

Table 2. Specific estimates and predictions of the Hubble constant H_0 for some galaxies.

Galaxy	Measurements (receiver (1), MW)				Model **prediction** (from rotational velocities and equations)					
Transmitter (2)	$v_2 - v_1$ (km/s)	$d_\odot$ (Mpc)	H_0 (km/s/Mpc) (from $\Delta v/d_o$)	ref	$v_{02} - v_{01}$ (km/s)	t_1' (Gy) (MW)	t_2' (Gy)	$d_{20} - d_{10}$ (Mpc)	$d_\odot$ (Mpc)	H_0 (km/s/Mpc)
CMB	c	**~4235** (13.861 ± 0.058) [Gy])	**68.3 ± 1.5**	[5]	c	0.52	0.0004	159.3	4387 (14.31 [Gy])	**68.32**
UGC12591	6945 ± 3	X = 120 σ = 40 **68 to 167** 5 values	57.9 min/max **41.6 to 102.1**	NED	6942 (−10%) (+10%	0.52	0.46	0.42	94.1	**73.703 (73.705) (73.701)**
COMA cluster	6995 ± 39	X = 109.3 σ = 26 ($h_{-1} = 0.705$) **77 to 144** 10 values	64.0 min/max **51.5 to 84.7**	NED	7016	0.52	~1 (0.5 × 2) See **Figure 3**	3.44	95.16	**73.49**
UDG 44 Dragonfly	6391 ± 6	X = **94.4** ($h_{-1} = 0.678$) **±6** 10 values	67.7 min/max **61.1 to 72.3**	NED	6393	0.52	0.57	0.32	86.7	**73.65**
UGC2885	5801 ± 3	X = 83.7 ($h_{-1} = 0.678$) **±6** **54 to 80.6** 3 values	69.3 **64.6 to 74.7** Or min/max **71.9 to 107.5**	NED SIMBAD	5810	0.52	~0.75 (0.5 × 1.4)	1.36	78.84	**73.57**
AGC114905	5435 ± 14	X = **75.6** ($h_{-1} = 0.678$) **±5.3**	71.9 min/max **67.1 to 77.3**	NED	5455	0.52	~0.575 (0.5 × 1.15)	0.48	73.99	**74.44**
NGC4183	929 ± 1	X = 16.0 σ = 3 **9.8 to 24.6** 33 values	58.0 min/max **37.7 to 94.9**	NED	935	0.52	0.67	0.14	12.68	**73.23**
DDO161	543	$6.03 \pm^{0.29}_{0.21}$	90.0	TRGB [25]	740	0.52	0.46	−0.04	10.05	**73.90**
	742 ± 2	**4.7 to 7.3** 12 value	min/max **101 to 158**	NED						
	743	10.6	70	HI [26]						
	-	X = **9.4**	75.0	HI [27]						
NGC3198	681 ± 1	X = 13 ± **0.95** 52 values	52.3 min/max **48.7 to 56.6**	NED	681.3	0.52	~0.53 (0.5 × 1.06)	0.007	9.24	**73.63**
	649 to 684 16 values	12 to 17 14 value	min/max **38 to 57**	SIMBAD						

Continued

NGC253	243 ± 1	X = 3.59 ± 0.25 **2.1 to 4.27** 23 values	67.7 min/max **56.7 to 118**	NED	242 (−10%) (+10%)	0.52	0.5	0.005	3.28 (2.94) (3.61)	**73.907** **(73.933)** **(73.886)**
	1284 ± 5	X = 23.8 ± 1.7 9.2 to 29.1 118 values	53.9 min/max **50.1 to 58.3**	NED						
M87					1280	0.52	0.44	−0.10	17.38	**73.85**
	1284 ± 5	**16.7** ± 0.9	76.9 min/max **72.7 to 81.6**	TRGB [28]						

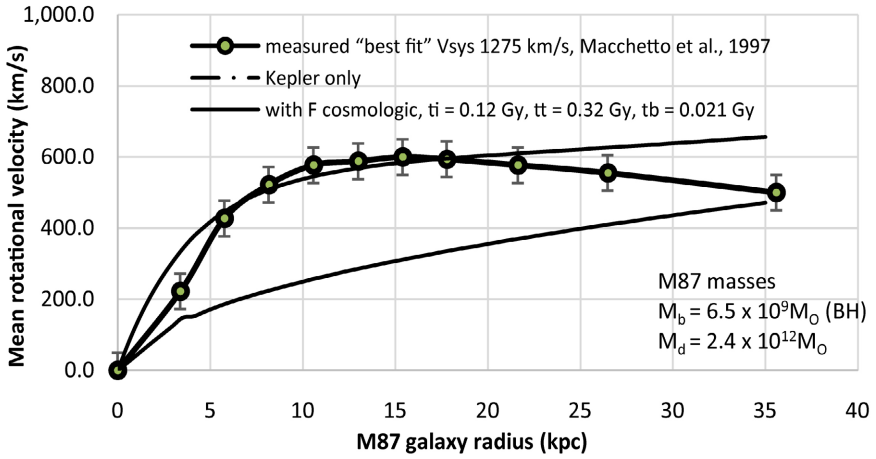

Figure 11. M87 rotational velocities.

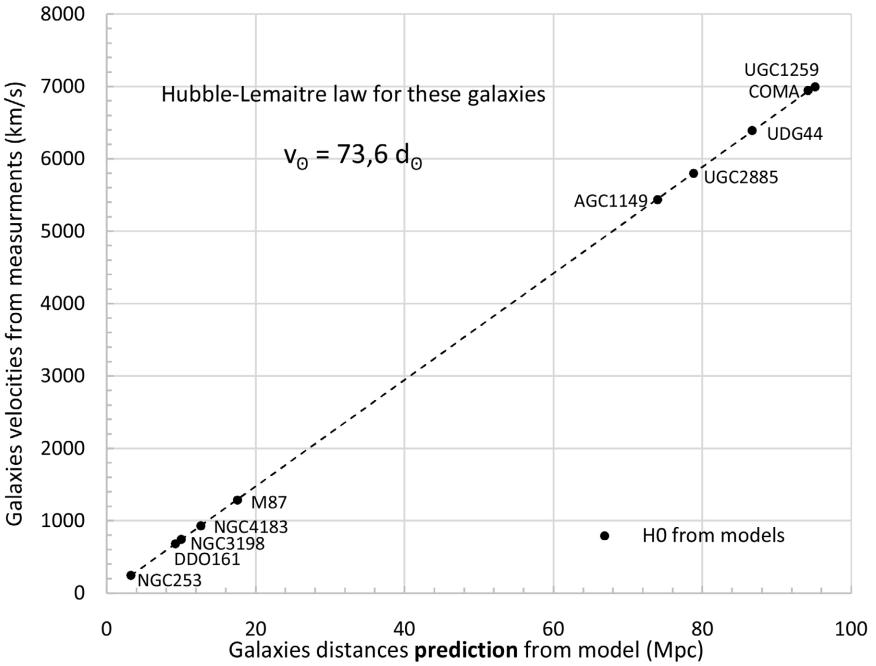

Figure 12. Theoretical Hubble-Lemaître law using measured recession velocity of studied galaxies and predicted distance $d_{\odot}$ using the model.

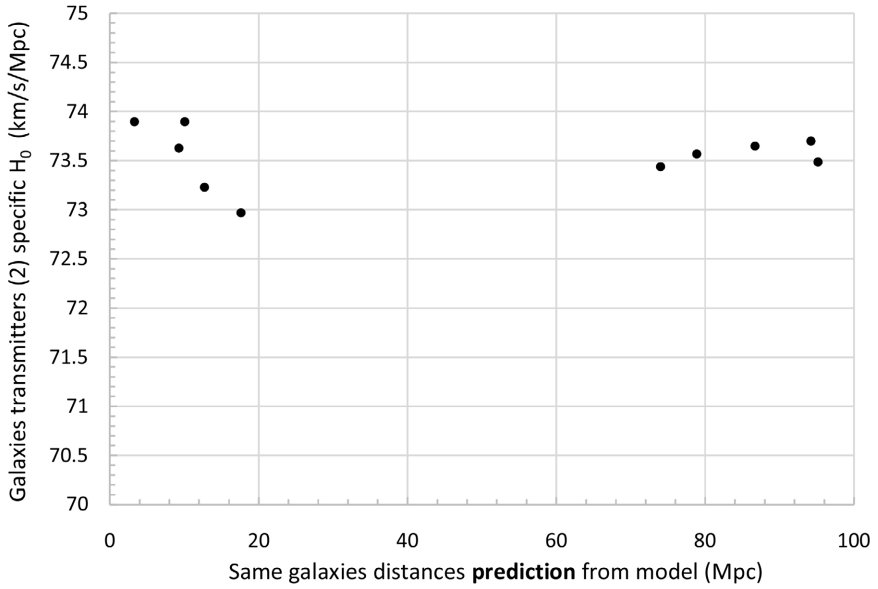

Figure 13. Specific predicted H_0 of studied galaxies vs predicted distance $d_\odot$ using the model.

3) In order to estimate the galaxies peculiar velocity effects [29], we increased and decreased the velocities $v_2 - v_1$ of NGC253 galaxy by ±10% (z ~0.00081) and UGC12591 (z ~0.0231). There is a very small variation in H_0.

We can plot for these galaxies the theoretical Hubble-Lemaître law according to the predictions as shown in **Figure 12**. We obtain a linear fit value of 73.6 σ 0.3 [km/s/Mpc]. This value can be compared to that obtained by Pantheon+ and SH0ES [30] (LCDM, flat, z = 0.001 to 2.26) 73.6 +/− 1 [km/s/Mpc]. Also, with the value of COSMOFLOW-3 study [31] of more than 17,000 galaxies located at ~1 - 250 [Mpc]. The estimated mean value of the Hubble constant is 75 ± 2 [km/s/Mpc]. In **Figure 13**, we see the specific value of the constant H_0 (*MW*, galaxy) as obtained according to the model. We see that this value varies depending on the galaxy being observed. In addition, the values are all around 73 - 74, *i.e.* for galaxies formed around 0.4 to 0.8 [Gy] after the SB (slow bang).

6. Discussions

In order to demonstrate the effects of each of the main parameters that influence the prediction of the Hubble constant, *i.e.*, the difference in the velocities of galaxies $v_2 - v_1$, the formation time of the observed galaxy (transmitter) t_2', we used the parameters of the galaxy M87, namely:

M87: $v_2 - v_1 = 1284$, $v_{02} - v_{01} = 1280$, $t_2' = 0.44$, $d_{20} - d_{10} = -0.1$, $d_\odot = 17.3$, $H_0 = 73.85$.

If we delay the formation time of M87 by 0.3 [Gy], we get,

M87: $v_2 - v_1 = 1284$, $v_{02} - v_{01} = 1293$, $t_2' = 0.74$, $d_{20} - d_{10} = 0.29$, $d_\odot = 17.5$, $H_0 = 73.21$.

If we increase the relative velocity of M87 by 2000 [km/s], we get,

M87: $v_2 - v_1 = 3284$, $v_{02} - v_{01} = 3280$, $t_2' = 0.44$, $d_{20} - d_{10} = -0.26$,

$d_{\odot} = 44.5$, $H_0 = 73.74$.

If we decrease the relative velocity of M87 by 1000 [km/s], we get,

M87: $v_2 - v_1 = 284$, $v_{02} - v_{01} = 280$, $t_2' = 0.44$, $d_{20} - d_{10} = -0.08$, $d_{\odot} = 3.8$, $H_0 = 74.46$.

We see that each of the parameters makes the Hubble constant vary in plus or minus. In this case, the variation ranges from −0.64 to +0.61.

In summary, if we make several positive and negative variations of the mentioned parameters, we observe the following effects related to the observations made from the MW.

- An increase in the observed galaxy formation time (more towards LTG) produces a decrease of H_0.
- A decrease in the formation time of the observed galaxy (more towards ETG) produces an increase of H_0.
- An increase in the relative velocity of the galaxy produces an increase in relative distance which results in a small decrease in H_0.
- A decrease in the relative velocity of the galaxy produces a decrease in the relative distance which results in a small increase in H_0.

7. Conclusions

We have seen in this article that a model of Hubble-Lemaître law using the notion of a transmitter (galaxy) and a receiver (MW) coupled to a universe model (Slow Bang Model, SB), based on a quantum approach to the evolution of space-time as well as on an equation of state that retains all the infinitesimal terms, has made it possible to explain why we measure different values of the Hubble constant H_0. Indeed, we have seen that this constant depends on the transceiver pair and that it can vary from the lowest observable value, that of the photons of the CMB (theoretical $\sim 68.32^{+0.49}_{-0.47}$ [km/s/Mpc]) to increasingly higher values depending on the later origin of the formation of the observed galaxy (or cluster). We have produced a theoretical table of the values of the constant according to the possible pairs of transmitter/receiver in the case where these follow the Hubble flow without disturbance. The calculated values of the constant are in the order of magnitude of all values mentioned in past studies. Subsequently, we applied the models to the case of 9 galaxies and COMA cluster and found that the models predict acceptable values of their distances and Hubble constant since these galaxies mainly follow the Hubble flow rather than the effects of a galaxy cluster or a group of clusters. In conclusion, we affirm that this Hubble tension does not really exist and it is rather the understanding of the meaning of this constant that is rather questioned.

Finally, we believe that the models developed seem interesting and we hope that it will arouse future interest.

Funding Statement

Funding for this article was supported by the University of Quebec at Chicoutimi.

Acknowledgements

The author would like to thank the members of his family, especially his spouse (Danielle) who with patience to bear this work as well his children (Pierre-Luc, Vincent, Claudia), for their encouragement to persevere despite the more difficult periods. Finally, thanks to the University of Quebec at Chicoutimi and to the colleagues of the Department of Applied Sciences for their supports in the realization of this work.

Conflicts of Interest

The author declares that there is no conflict of interest regarding the publication of this paper.

References

[1] Di Valentino, E., Mena, O., Pan, S., Visinelli, L., Yang, W., Melchiorri, A. and Silk, J. (2021) In the Realm of the Hubble Tension—A Review of solutions. *Classical and Quantum Gravity*, **38**, Article ID: 153001. https://doi.org/10.1088/1361-6382/ac086d

[2] Hu, J.P. and Wang, F.Y. (2023) Hubble Tension: The Evidence of New Physics. *Universe*, **9**, 94. https://doi.org/10.3390/universe9020094

[3] Collaboration, P., Aghanim, N., Akrami, Y., Alves, M.I.R., Ashdown, M., Aumont, J. and Bielewicz, P. (2020) Planck 2018 Results. *A&A*, **641**, A12. https://doi.org/10.1051/0004-6361/202039265

[4] Xiang, M. and Rix, H.W. (2022) A Time-Resolved Picture of Our Milky Way's Early Formation History. *Nature*, **603**, 599-603. https://doi.org/10.1038/s41586-022-04496-5

[5] Balkenhol, L., Dutcher, D., Mancini, A.S., Doussot, A., Benabed, K., Galli, S. and SPT-3G Collaboration (2023) Measurement of the CMB Temperature Power Spectrum and Constraints on Cosmology from the SPT-3G 2018 TT, TE, and EE Dataset. *Physical Review D*, **108**, Article ID: 023510. https://doi.org/10.1103/PhysRevD.108.023510

[6] Perron, J. (2019) An Alternative to Hidden Matter? A Cosmological Model of Galaxy Rotation Using Cosmological Gravity Force, F_Λ (ALW). https://doi.org/10.20944/preprints201905.0335.v1

[7] Perron, J. (2021) An Alternative to Hidden Matter? Part 1: The Early Universe (t_p to 10^{-9} s), Energy Creation the Alphaton, Baryogenesis. *Journal of High Energy Physics, Gravitation and Cosmology*, **7**, 784-807. https://doi.org/10.4236/jhepgc.2021.73046

[8] Perron, J. (2021) An Alternative to the Hidden Matter? Part 2: A Close Universe (10^{-9} s to 3 Gy), Galaxies and Structures Formation. *Journal of High Energy Physics, Gravitation and Cosmology*, **7**, 808-843. https://doi.org/10.4236/jhepgc.2021.73047

[9] Perron, J. (2021) An Alternative to Hidden Matter? Part 3: An Open Universe (3 Gy to 76 Gy) Galaxies and Structures Rotation. *Journal of High Energy Physics, Gravitation and Cosmology*, **7**, 844-872. https://doi.org/10.4236/jhepgc.2021.73048

[10] Perron, J. (2023) ETG Galaxies (<400 [My]) from JWST Already Predicted in 2019 from This Cosmological Model AΛΩ (Slow Bang Model, SB) *Journal of High Energy Physics, Gravitation and Cosmology*, **9**, 800-834. https://doi.org/10.4236/jhepgc.2023.93063

[11] Aghanim, N., Akrami, Y., Arroja, F., Ashdown, M., Aumont, J., Baccigalupi, C. and Pettorino, V. (2020) Planck 2018 Results-I. Overview and the Cosmological Legacy of Planck. *Astronomy & Astrophysics*, **641**, A1. https://doi.org/10.1051/0004-6361/202039265

[12] Blitz, L., Fich, M. and Stark, A.A. (1980) The Galactic Rotation Curve to R = 18 KPC. *Symposium-International Astronomical Union*, Vol. 87, 213-220. https://doi.org/10.1017/S0074180900072582

[13] Giovanelli, R., Haynes, M.P., Rubin, V.C. and Ford Jr., W.K. (1985) UGC 12591—The Most Rapidly Rotating Disc Galaxy. *The Astrophysical Journal*, **301**, L7-L11. https://doi.org/10.1086/184613

[14] Kent, S.M. and Gunn, J.E. (1982) The Dynamics of Rich Clusters of Galaxies. I, the Coma Cluster. *The Astronomical Journal*, **87**, 945-971. https://doi.org/10.1086/113178

[15] Rood, H.J., Page, T.L., Kintner, E.C. and King, I.R. (1972) The Structure of the Coma Cluster of Galaxies. *The Astrophysical Journal*, **175**, 627-647. https://doi.org/10.1086/151585

[16] Chincarini, G. and Rood, H.J. (1975) Size of the Coma Cluster. *Nature*, **257**, 294-295. https://doi.org/10.1038/257294a0

[17] Van Dokkum, P., Wasserman, A., Danieli, S., Abraham, R., Brodie, J., Conroy, C. and Villaume, A. (2019) Spatially Resolved Stellar Kinematics of the Ultra-Diffuse Galaxy Dragonfly 44. I. Observations, Kinematics, and Cold Dark Matter Halo Fits. *The Astrophysical Journal*, **880**, Article No. 91. https://doi.org/10.3847/1538-4357/ab2914

[18] Gentile, G., Józsa, G.I.G., Serra, P., Heald, G.H., de Blok, W.J.G., Fraternali, F. and Oosterloo, T. (2013) HALOGAS: Extraplanar Gas in NGC 3198. *Astronomy & Astrophysics*, **554**, A125. https://doi.org/10.1051/0004-6361/201321116

[19] Mancera Piña, P.E., Fraternali, F., Oosterloo, T., Adams, E.A., Oman, K.A. and Leisman, L. (2022) No Need for Dark Matter: Resolved Kinematics of the Ultra-Diffuse Galaxy AGC 114905. *Monthly Notices of the Royal Astronomical Society*, **512**, 3230-3242. https://doi.org/10.1093/mnras/stab3491

[20] Martins, C. F. and Salucci, P. (2007) Analysis of Rotation Curves in the Framework of R n Gravity. *Monthly Notices of the Royal Astronomical Society*, **381**, 1103-1108. https://doi.org/10.1111/j.1365-2966.2007.12273.x

[21] Stark, D.V., McGaugh, S.S. and Swaters, R.A. (2009) A First Attempt to Calibrate the Baryonic Tully-Fisher Relation with Gas-Dominated Galaxies. *The Astronomical Journal*, **138**, 392-401. https://doi.org/10.1088/0004-6256/138/2/392

[22] Côté, S., Carignan, C. and Freeman, K.C. (2000) The Various Kinematics of Dwarf Irregular Galaxies in Nearby Groups and Their Dark Matter Distributions. *The Astronomical Journal*, **120**, 3027-3059. https://doi.org/10.1086/316883

[23] Pence, W.D. (1981) A Photometric and Kinematic Study of the Barred Spiral Galaxy NGC 253. II—The Velocity Field. *The Astrophysical Journal*, **247**, 473-483. https://doi.org/10.1086/159056

[24] Macchetto, F., Marconi, A., Axon, D. J., Capetti, A., Sparks, W. and Crane, P. (1997) The Supermassive Black Hole of M87 and the Kinematics of Its Associated Gaseous Disc. *The Astrophysical Journal*, **489**, 579-600. https://doi.org/10.1086/304823

[25] Karachentsev, I.D., Makarova, L.N., Tully, R.B., Rizzi, L., Karachentseva, V.E. and Shaya, E.J. (2017) DDO 161 and UGCA 319: An Isolated Pair of Nearby Dwarf Galaxies. *Monthly Notices of the Royal Astronomical Society: Letters*, **469**, L113-L117. https://doi.org/10.1093/mnrasl/slx061

[26] AL-Dahlaki MSc, H.H. (2021) Calculation and Comparison of Certain Physical Properties of Sample Irregular Galaxies with the Milky Way Galaxy. *Karbala International Journal of Modern Science*, **7**, Article No. 12. https://doi.org/10.33640/2405-609X.3163

[27] Begeman, K.G. (1989) HI Rotation Curves of Spiral Galaxies. I-NGC 3198. *Astronomy and Astrophysics*, **223**, 47-60.

[28] Bird, S., Harris, W.E., Blakeslee, J.P. and Flynn, C. (2010) The Inner Halo of M 87: A First Direct View of the Red-Giant Population. *Astronomy & Astrophysics*, **524**, A71. https://doi.org/10.1051/0004-6361/201014876

[29] Davis, T.M., Hui, L., Frieman, J.A., Haugbølle, T., Kessler, R., Sinclair, B., *et al.* (2011) The Effect of Peculiar Velocities on Supernova Cosmology. *The Astrophysical Journal*, **741**, 67. https://doi.org/10.1088/0004-637X/741/1/67

[30] Brout, D., Scolnic, D., Popovic, B., Riess, A.G., Carr, A., Zuntz, J., *et al.* (2022) The Pantheon+ Analysis: Cosmological Constraints. *The Astrophysical Journal*, **938**, 110. https://doi.org/10.3847/1538-4357/ac8e04

[31] Tully, R.B., Courtois, H.M. and Sorce, J.G. (2016) COSMICFLOWS-3. *The Astronomical Journal*, **152**, Article No. 50. https://doi.org/10.3847/0004-6256/152/2/50